

Statistical constraints on non-cosmological subclasses of GRBs

Yana Tikhomirova,^{1,2*} Boris E. Stern^{3,1,2*} and Roland Svensson^{2*}

¹*Astro Space Centre of Lebedev Physical Institute, 84/32 Profsojuznaja Street, Moscow 117997, Russia*

²*SCFAB, Stockholm Observatory, Department of Astronomy, SE-106 91 Stockholm, Sweden*

³*Institute for Nuclear Research of Russian Academy of Sciences, 7a, Prospect 60-letija Oktjabrja, Moscow 117312, Russia*

Accepted, Received

ABSTRACT

There still exists the possibility that the phenomenon of gamma-ray bursts (GRBs) is a mixture of events of different nature, even within the class of long (>2 s) bursts. We try to put statistical constraints on a possible non-cosmological component using the uniform GRB catalog of Stern & Tikhomirova[#] obtained from an overall scan of the full 9.1 year BATSE 1024 ms data. The sample consists of 3906 GRBs and includes non-triggered bursts with peak fluxes down to $0.1 \text{ photons cm}^{-2} \text{ s}^{-1}$. We find no significant deviations from isotropy. The constraints on a non-cosmological population are still weak. The allowed contribution of a GRB subpopulation originating from an extended galactic halo is $\sim 60\%$ and the upper limit on an Euclidian component (e.g., nearby galactic or non-cosmological extragalactic GRBs) is 23% . The results concern mainly the class of long GRBs.

Key words:

1 INTRODUCTION

At present there are direct redshift measurements for 23 Gamma-Ray Bursts[&]. All of them are cosmological. If we believe that all GRBs are of the same nature, then we must reject all non-cosmological models of GRBs and to close this issue.

However, first we should mention that long (>2 s) and short (<2 s) GRBs are probably events of different nature (Kouveliotou et al. 1993) and all of the redshift measurements have been done only for long bursts. Moreover, the impression of the uniformity of GRBs could arise from their diversity whereas they can be a mixture of events of different origin even within the class of long bursts. For example, Horvath (1998) suggested the existence of an “intermediate” class of GRBs with durations of several seconds and softer spectra. The evidence for this is still not statistically convincing. Nevertheless such a possibility should not be discarded.

In this work, we revisit statistical studies of non-cosmological models which were done before the discovery of afterglows. Now we have a much larger statistics which will not be extended during the next few years. Therefore it is interesting to outline constraints on non-cosmological (i.e., local galactic, galactic halo, or low redshift extragalactic) GRB subpopulations which we can obtain from the present GRB sample. We concentrate only on those models which can provide a reasonable isotropy of GRBs and therefore we do not consider the galactic disk population (except for a very local one).

Previous attempts to constrain Galactic GRB scenarios (see, for example, Hakkila et al., 1994, Loredano & Wasserman, 1998) showed that the least constrained local model is an extended galactic halo of bursters. According to Hakkila et al. (1994), for some narrow range of parameters, all GRBs could originate from a galactic halo being still in agreement with the angular and the brightness distributions of GRBs as observed by the Burst And Transient Source Experiment (BATSE)(Fishman 1992).

It is also interesting to recalculate a possible Euclidean component (i.e., a population homogeneously distributed in Euclidean space). It could be represented by a local Galactic population at distances <500 pc or by extragalactic sources at $z \ll 1$. The estimate of Kommers et al. (2000) for the BATSE sample with peak fluxes down to $\approx 0.2 \text{ photons cm}^{-2} \text{ s}^{-1}$ is about 10% .

The deepest and largest GRB sample was found by search for non-triggered GRBs in the BATSE continuous records of Stern et al. (2000, 2001). Their new uniform catalog[#] (UC) includes 3906 (2068 triggered and 1838 non-triggered) events with peak fluxes down to $\approx 0.1 \text{ photons cm}^{-2} \text{ s}^{-1}$ (a factor 2 lower than the BATSE trigger threshold). Moreover, they applied a new method to measure the efficiency of the search which is important for the reconstruction of the real N -log P distribution.

Note, that all bursts of the UC were extracted from the DISCLA BATSE data of the 1024 ms time resolution. The bursts which can be classified as short (1 bin events) are about 12% in the sample. Therefore, **the constraints will concern mainly the class of long GRBs**. In §2, we present the results of a general test of the UC for large scale isotropy. We constrain the possible contribution of a halo population in §3, and of an Euclidean component in the GRB statistics in §4.

* E-mail: jana@anubis.asc.rssi.ru (YT); stern@lukash.asc.rssi.ru (BES); svensson@astro.su.se (RS)

[#] available at http://www.astro.su.se/groups/head/grb_archive.html

& see Greiner’ web page at <http://www.aip.de/jcg/grb.html>

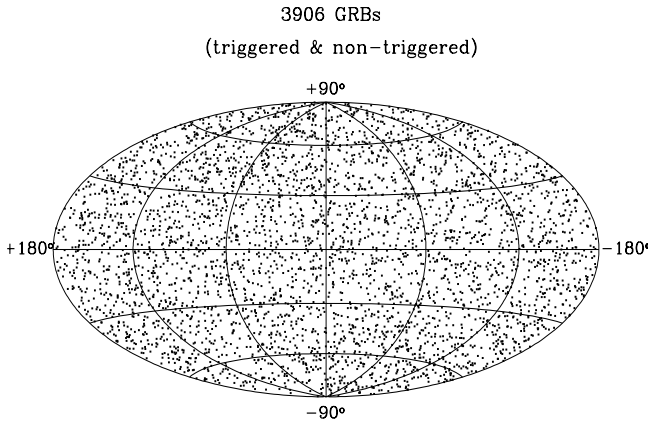


Figure 1. Sky distribution of the 3906 GRBs in the UC on an Aitoff-Hammer projection in Galactic coordinates.

2 TEST FOR ISOTROPY

The preliminary test of the UC for isotropy was done in Tikhomirova & Stern (2000). Here, we extend the analysis to the complete sample.

2.1 Statistical tests

Figure 1 shows the distribution of the locations of all UC GRBs in galactic coordinates. We use the following tests for the large scale isotropy (see Hartmann & Epstein 1989 for test 1) and Briggs 1993, 1994 for tests 2)-5)) :

1) The dipole vector \vec{R} :

$$\vec{R} = \frac{\sum_i \vec{r}_i}{N},$$

where \vec{r}_i is the unit vector in the direction of a GRB and N is the number of bursts in the sample. \vec{R} characterizes the dipole moment in a coordinate free way and tests for large scale anisotropy.

2) $\langle \cos(\theta) \rangle$, where θ is the angle between the Galactic center and a GRB. This quantity characterizes the dipole moment in the Galactic system and tests for a Galactic population.

3) $\langle \sin^2(b) - 1/3 \rangle$, where b is the Galactic latitude of a burst. This quantity characterizes the quadrupole moment in the Galactic system and tests for a local Galactic population.

4) $\langle \sin(\delta) \rangle$, where δ is the declination of a burst. and

5) $\langle \sin^2(\delta) - 1/3 \rangle$, which characterizes the dipole and quadrupole moments in the equatorial system and tests for systematic errors.

The statistical errors are $\sigma = (1/\sqrt{3N})$ for the components of \vec{R} and the tests 2) and 4); and $\sigma = (\sqrt{4}/\sqrt{45N})$ for the tests 3) and 5). The statistical error for the absolute value of \vec{R} is $\sigma = (1/\sqrt{N})$. The total error has an additional component associated with the errors of the locations of individual GRBs. Although the location accuracy for the UC GRBs is as low as several degrees (Tikhomirova & Stern 2000) this component is smaller by an order of magnitude than the statistical one as was checked using Monte-Carlo simulations.

2.2 Expected values

The values of $|\vec{R}|$ and of the statistics 2)-5) are zero for an isotropic distribution of bursts observed by an ideal instrument. The values corrected for the non-uniform BATSE sky exposure (Paciesas et al.

1999) are listed in the second column of Table 1. In the BATSE catalogs, these quantities usually have their expected values (see Paciesas et al. 1999). However, other systematic effects may appear as a result of a non-uniform burst selection. One such effect is caused by an active CygX-1, which reduces the efficiency of weak GRBs detected in that direction.

Such effects may be revealed by the test bursts used in the scan of Stern et al. (2000, 2001) to estimate the scan efficiency. Test bursts are initially isotropic and are subjected to the same systematic effects as real bursts. However, their statistics is limited (~ 5300). Therefore, we consider both the values expected for the BATSE sky exposure (column 2 in Table 1) and the values observed for test bursts (column 4 in Table 1).

2.3 Results

The results of the tests together with the 1σ statistical errors are listed in columns 4-7 of Table 1. The values for the 4Br catalog are given for comparison in column 3. (Note, that \vec{R} was not given in the 4Br catalog.) Test bursts show a marginally significant dipole (at the $\sim 2.5\sigma$ level) in the direction opposite to Cyg X-1, which is caused by a strong deficit of detected weak bursts in a cone $\sim 25^\circ$ around Cyg X-1. A similar effect appears for the sample of real GRBs.

Table 2 shows the deviations from the values expected for the BATSE exposure (columns 2-5) and from the values for test bursts (columns 6-8). The deviations from the value for the test bursts are given in units of σ determined as

$$\sigma = \sqrt{\sigma_{\text{test bursts}}^2 + \sigma_{\text{real bursts}}^2}. \quad (1)$$

All deviations are within 1.5σ so the results of the tests are consistent with isotropy.

We also checked the excess of bursts towards M31 for the full sample in the UC as well as for only weak (< 0.4 photons $\text{cm}^{-2} \text{s}^{-1}$) bursts. There is no excess.

3 TEST FOR AN EXTENDED GALACTIC HALO SUBPOPULATION OF GRB SOURCES

3.1 The Model for an Extended Halo of GRB sources

The traditional model of a halo is associated with old neutron stars which have been ejected from the galactic disk (Shklovskii & Mitrofanov 1985). The test for an extended halo population is based on the displacement of the Solar system from the Galactic center (8.5 kpc) and the presence of the nearby galaxy M31 (670 kpc away) which should have a similar extended halo. Then we must check two things: the dipole moment in the direction of the Galactic center and the excess of bursts around M31. The larger the halo of bursters, the smaller is the dipole moment but then GRBs from M31 become more visible. The same logic was used in previous works (e.g., Hakkila et al., 1994).

In the approximation of a steady outflow of neutron stars, we have a spatial distribution of bursters with a Coulomb-like tail and a core:

$$N(r) = N_0 r_c^2 / (r_c^2 + r^2), \quad (2)$$

where $N(r)$ is the burster density per unit volume, N_0 is the density at the center, r is the distance from the Galactic center, and r_c is the core size. The distribution should decline faster than $1/r^2$ at some r because a neutron star cannot emit GRBs for an infinite

Table 1. Results of the large scale isotropy test.

statistics	expected for isotropy	4Br catalog (1637)*	UC			
			test bursts (5345)*	all bursts (3906)*	triggered (2068)*	non-triggered (1838)*
$ \vec{R} $	0.018	0.029 ± 0.025	0.026 ± 0.014	0.021 ± 0.016	0.020 ± 0.022	0.030 ± 0.023
R1	0.000	0.005 ± 0.014	-0.022 ± 0.008	-0.012 ± 0.009	-0.006 ± 0.013	-0.019 ± 0.013
R2	0.000	0.015 ± 0.014	0.014 ± 0.008	0.014 ± 0.009	0.005 ± 0.013	0.024 ± 0.013
R3	0.018	0.024 ± 0.014	0.003 ± 0.008	0.010 ± 0.009	0.019 ± 0.013	-0.000 ± 0.013
$\langle \cos(\theta) \rangle$	-0.009	-0.025 ± 0.014	-0.012 ± 0.008	-0.016 ± 0.009	-0.013 ± 0.013	-0.019 ± 0.013
$\langle \sin^2(b) - 1/3 \rangle$	-0.004	-0.001 ± 0.007	0.001 ± 0.004	-0.007 ± 0.005	-0.007 ± 0.007	-0.006 ± 0.007
$\langle \sin(\delta) \rangle$	0.018	0.024 ± 0.014	0.003 ± 0.008	0.010 ± 0.009	0.019 ± 0.013	-0.000 ± 0.013
$\langle \sin^2(\delta) - 1/3 \rangle$	0.024	0.025 ± 0.007	0.022 ± 0.004	0.025 ± 0.005	0.024 ± 0.007	0.026 ± 0.007

* the number of events in each sample

Table 2. Deviations from the expected values for large scale isotropy.

statistics	deviation from the value expected for the isotropy				deviation from the value for the test bursts		
	4Br catalog	UC			UC		
		all	trig.	non-tr.	all	trig.	non-tr.
\vec{R}^*	0.7σ	1.2σ	0.3σ	1.5σ	0.6σ	0.9σ	0.4σ
$\langle \cos(\theta) \rangle$	$-1.1\sigma^{**}$	-0.7σ	-0.3σ	-0.8σ	-0.3σ	-0.1σ	-0.5σ
$\langle \sin^2(b) - 1/3 \rangle$	$+0.4\sigma^{**}$	-0.5σ	-0.5σ	-0.2σ	-1.1σ	-1.0σ	-0.8σ
$\langle \sin(\delta) \rangle$	$+0.4\sigma^{**}$	-0.9σ	$+0.1\sigma$	-1.3σ	$+0.6\sigma$	$+1.1\sigma$	-0.2σ
$\langle \sin^2(\delta) - 1/3 \rangle$	$+0.1\sigma^{**}$	$+0.2\sigma$	$+0.0\sigma$	$+0.3\sigma$	$+0.5\sigma$	$+0.3\sigma$	$+0.5\sigma$

* deviation of the vector

** Paciesas et al. (1999)

time or just because of the finite age of the Galaxy. Expression (2) gives a suitable asymptotic slope of the $\log N - \log P$ distribution: $dN/d(\log P) \propto P^{-\alpha}$ with $\alpha = 0.5$ for small brightnesses P in agreement with the observed data (Kommers et al. 2000, Stern et al. 2001).

We assumed identical halos for both our Galaxy and M31 and tried two cutoffs for the distribution (2): at 300 kpc (i.e., halfway between the Galaxy and M31) and at 800 kpc which could represent the case of an infinite distribution (we are within the M31 halo in this case). This rough model seems to be sufficient for an approximate estimate.

The GRB luminosity function was assumed to be a lognormal distribution:

$$dN/dL = \exp[-\log^2(L/L_0)/\sigma_L^2], \quad (3)$$

where L is the GRB peak luminosity, L_0 is the average GRB peak luminosity, and σ_L is the width of the GRB luminosity function.

The model distributions of GRBs were obtained using Monte-Carlo simulations. The variable parameters were: the core radius, r_c , the average GRB peak luminosity, L_0 , and the width of the GRB luminosity function, σ_L . The averaged peak luminosity L_0 was expressed as P_{100} measured in units of $2 \cdot 10^{41} \text{ erg s}^{-1}$ in the 50 - 300 keV energy range. This is the luminosity which produces a flux of 1 photon $\text{s}^{-1} \text{ cm}^{-2}$ at a distance of 100 kpc ($L_0 \approx 2 \times 10^{41} P_{100}$).

The spatial distribution of GRBs was sampled according to (2), where r is the distance of a GRB from the center of the Galaxy or from the center of M31 (with equal probabilities). The locations of GRBs on the sky were sampled imposing experimental location errors depending on the "observed" brightness. The intrinsic peak brightness of a GRB was sampled according to equation (3). The "observed" distribution of simulated GRBs was folded with the BATSE exposure function (Paciesas et al., 1999) and with the detection efficiency determined using the test bursts method of Stern et al. (2000, 2001).

3.2 The constraints on the halo subpopulation

We represented the full sample of GRBs as $(\xi - 1)S_0 + \xi S_h$ where S_0 is an isotropic subsample (presumably cosmological) with an unknown $\log N - \log P$ distribution, and S_h is the model halo subsample. We want to determine the value of the halo fraction ξ for which the following four criteria are satisfied:

- (i) The dipole moment, D_g , towards the Galactic center should be within the observed 2σ upper limit: $C_g = 0.009$
- (ii) The fraction of bursts with locations within 25° from the M31 location, N_{25} , should not exceed the observed 2σ upper limit which is $C_{25} = (N_{\text{real}} - N_{\text{exp}} + 2\sigma)/N_{\text{real}} = 0.14$
- (iii) The same should apply for an 18° region around M31, for N_{18} : $C_{18} = 0.21$
- (iv) The $\log N - \log P$ distribution should be consistent with the observed one:
 - the sum of the distributions for subsamples S_0 and S_h should give the observed one,
 - the distribution of the subsample S_0 should be smooth, i.e., the difference between neighbouring points should not exceed 3σ , and
 - the distribution of S_0 should not bend down too sharply at low brightnesses, i.e., not steeper than $dN/d(\log P) \propto P^{+0.5}$ (see Fig. 2). This limiting slope corresponds to a reasonably sharp turnover of the $\log N - \log P$ distribution at its dim end.

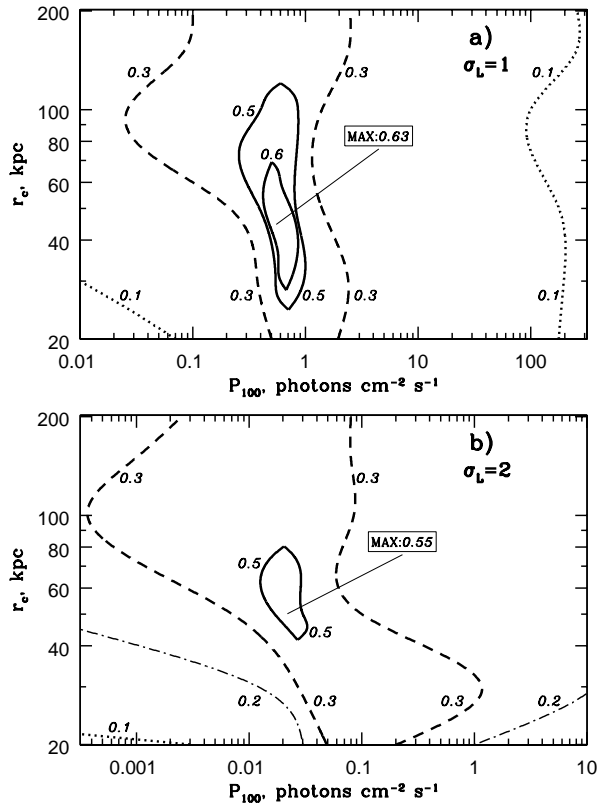


Figure 2. Maps of constant levels of the allowed fraction ξ of the halo subpopulation in the whole sample of the UC: a) for $\sigma_L = 1$, b) for $\sigma_L = 2$. r_c is the halo core radius, and P_{100} is the GRB peak count rate at a distance of 100 kpc.

For the observed distribution, we used the $\log N - \log P$ curve corrected for the detection efficiency of the scan of Stern et al. (2001). All limits were calculated for the full sample of the UC (3906 GRBs with peak fluxes down to 0.1 photons $\text{cm}^{-2} \text{ s}^{-1}$).

We searched for the fraction ξ at which the full model sample of GRBs satisfies all four criteria. For the first three criteria, ξ is just the minimum of the ratios C_g/D_g , C_{25}/N_{25} , and C_{18}/N_{18} .

We also tried to apply criteria 2 and 3 for weak bursts only (with peak fluxes < 0.4 photons $\text{cm}^{-2} \text{ s}^{-1}$). This case does not give stronger constraints.

3.3 Results

Comparing results for different halo cutoffs, we found that all constraints are slightly stronger for the 300 kpc cutoff. Here we present the results for the 800 kpc cutoff only, as it represents the case of an infinite halo and gives more conservative constraints.

The hypothesis that all GRBs originate from a Galactic halo is inconsistent with the data for any parameters. However, this fact is only of academic interest as observations of GRB afterglows showed that at least a substantial part of GRBs has a cosmological origin.

The results of the Monte-Carlo simulations for different parameters: r_c , see equation (2), P_{100} , and σ_L , see equation (3), are shown in Figure 2 as maps of isocontours of the allowed halo fraction ξ . The highest allowed fraction ξ is 0.63 for $\sigma_L = 1$ and 0.55 for $\sigma_L = 2$ (for $\sigma_L = 0$, $\xi = 0.7$, but the case of $\sigma_L = 0$, i.e.,

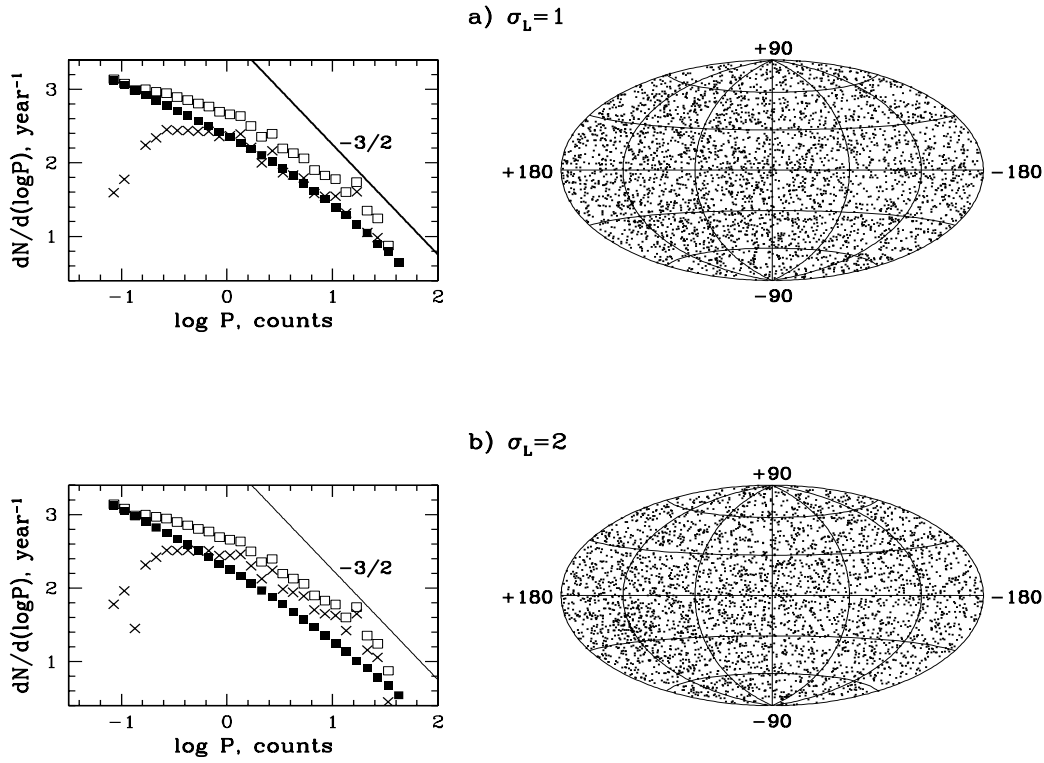


Figure 3. The simulated distributions for the case of maximum halo fraction ξ : a) for $\sigma_L = 1$, b) for $\sigma_L = 2$. Panels on the left, the $\log N - \log P$ distributions: the empty squares represent the observed data according to the UC, the filled squares represent the halo population, and the crosses correspond to the cosmological population. Panel on the right, the sky distribution: the whole sample (cosmological + halo). The halo of M31 is visible only for $\sigma_L = 2$. M31 is located at $l \approx 122^\circ$ and $b \approx -21^\circ$, on an Aitoff-Hammer projection in Galactic coordinates

for a standard candle GRB luminosity, is hardly realistic, and we do not discuss it further). The brightness intervals where the fraction of the galactic subpopulation can exceed 0.5 are limited to: $0.3 < P_{100} < 1.0$ for $\sigma_L = 1$ and $0.012 < P_{100} < 0.03$ for $\sigma_L = 2$. In terms of the average peak luminosity these intervals are $(1.0 - 3.3) \times 10^{41} \text{ erg s}^{-1}$ and $(1.8 - 4.5) \times 10^{40} \text{ erg s}^{-1}$, respectively (note the difference between arithmetical mean and logarithmic mean for the case of lognormal distribution).

The total rate of GRB events in the halo required to reproduce the observed GRB data depends on σ_L . In the case of $\sigma_L = 1$, the rate of GRBs out to 800 kpc should be ~ 8000 per year ($N_0 = 0.004 \text{ kpc}^{-3}$). In the case $\sigma_L = 2$, this number is $\sim 45\,000$ ($N_0 = 0.02 \text{ kpc}^{-3}$). Nevertheless, the total power emitted in the form of GRBs implied in the two cases is almost the same: $\sim 2 \cdot 10^{45} T \text{ erg year}^{-1}$, where T is the average duration of GRBs (a reasonable estimate is $T \sim 10 \text{ s}$). In both cases, M31 is at the edge of the sampling volume. The concentration of GRBs around the M31 location should be still visible for $\sigma_L = 2$ and hardly visible for $\sigma_L = 1$ (see Fig. 3).

4 CONSTRAINTS ON THE EUCLIDEAN SUBPOPULATION

We used the same logic as in §3 to constrain the possible fraction of a GRB subpopulation homogeneously distributed in space (the Euclidean component).

We represent the whole sample of GRBs as $(\xi - 1)S_0 + \xi S_e$, where S_0 is an isotropic subsample (presumably cosmological) with an unknown $\log N - \log P$ distribution, S_e is the homoge-

neous (in Euclidean space) subsample, and ξ is the possible fraction of GRBs of the homogeneous subsample in the full sample. For constraining ξ , we used only criterion 4 from §3.2.

The upper limit on an Euclidean component is 23% for the full sample of the UC (3906 GRBs with peak fluxes down to $0.1 \text{ photons cm}^{-2} \text{ s}^{-1}$). For the sample from the UC with peak fluxes down to the BATSE trigger threshold ($\approx 0.2 \text{ photons cm}^{-2} \text{ s}^{-1}$), the limit is about 14%. The same estimate of Kommers et al. (2000) is about 10%. They used their $\log N - \log P$ distribution with fluxes down to about $0.18\text{--}0.20 \text{ photons cm}^{-2} \text{ s}^{-1}$ and the difference in the constraints on the Euclidean component results from the difference in the estimates of $\log N - \log P$ distribution. Kommers' estimate for the number of dim GRBs is lower.

This constraint on the Euclidean component should be applied to any kind of local Galactic GRB subpopulation ($r < 300 \text{ pc}$) and to extragalactic sources at small redshifts ($z \ll 1$). If the sample of GRBs has a $\sim 20\%$ fraction of an Euclidean subpopulation, then this population dominates among weak GRBs. If this subpopulation is intrinsically different, it can be revealed in correlations between some GRB properties and the brightness.

5 CONCLUSIONS

The general results of our analysis of the new uniform catalog of GRBs can be formulated as follows:

- the large scale isotropy of the GRB sky distribution is confirmed for the larger and deeper sample of 3906 BATSE GRBs with peak fluxes down to $\approx 0.1 \text{ photons cm}^{-2} \text{ s}^{-1}$;
- the possible fraction of GRBs from an extended galactic halo

can be up to $\sim 60\%$. This is, however, only for narrow intervals of the parameters;

-the Euclidean component limited by a fraction of GRBs above the threshold $0.1 \text{ photons cm}^{-2} \text{ s}^{-1}$ is about 23%.

These constraints are still weak, so a considerable fraction of even long GRBs can be prescribed to some kind of a non-cosmological source population. Stronger constraints can hardly be obtained within the framework of the statistical approach. We believe that tighter constraints can be imposed from future afterglow observations.

Acknowledgement

This work was supported by the Swedish Natural Science Research Council, the Royal Swedish Academy of Science, the Wenner-Gren Foundation for Scientific Research, and the Russian Foundation for Basic Research (grant 00-02-16135).

REFERENCES

- Briggs, M. S. 1993, *ApJ*, 407, 126
- Briggs, M. S., Paciesas, W. S., Brock, M. N., Fishman, G. J., Meegan, C. A., Wilson, R. B. 1994, in *AIP Conf Proc.* 307, *Gamma-Ray Bursts*, ed. Fishman, G. J. (New York: AIP), 44
- Fishman, G. J. 1992, in *AIP Conf Proc.* 280, *Compton Gamma Ray Observatory*, eds. M. Friedlander, N. Gehrels, D. J. Macomb (New York: AIP), 669
- Hakkila, J., Meegan, C. A., Pendleton, G. N., Fishman, G. J., Wilson, R. B., Paciesas, W. S., Brock, M. N., Horack, J. M. 1994, *ApJ*, 422, 659
- Hartmann, D., Epstein, R. I. 1989, *ApJ*, 346, 960
- Horvath I. 1998, *ApJ*, 508, 757.
- Kommers, J. M., Lewin, W. H. G., Kouveliotou, C., van Paradijs, J., Pendleton, G. N., Meegan, C. A., Fishman, G. J., 2000, *ApJ*, 533, 696.
- Kouveliotou, C., Meegan, C. A., Fishman, G. J., Bhat, N. P., Briggs, M. S., Koshut, T. M., Paciesas, W. S., Pendleton, G. N. 1993, *ApJ*, 413, L101
- Lored, T. J., Wasserman, I. M. 1998, *ApJ*, 502, 75
- Paciesas, W. S. et al. 1999, *ApJS*, 122, 465
- Shklovskii, I. S., Mitrofanov, I. G. 1985, *MNRAS*, 212, 545
- Stern, B. E., Tikhomirova, Ya., Stepanov, M., Kompaneets, D., Berezhnoy, A., Svensson, R. 2000, *ApJL*, 540, L21.
- Stern, B.E., Tikhomirova, Ya., Kompaneets, D., Svensson, R., Poutanen, J. 2001, *ApJ*, 563, 80
- Tikhomirova, Ya., Stern, B.E. 2000, *Astronomy Letters*, 26, 672